Inorganic Chemistry

ARTICLE

pubs.acs.org/IC

Exploring the Metal Coordination Properties of the Pyrimidine Part of Purine Nucleobases: Isomerization Reactions in Heteronuclear Pt^{II}/Pd^{II} of 9-Methyladenine

Susana Ibáñez,[†] Francisca M. Albertí,[†] Pablo J. Sanz Miguel,[*,‡] and Bernhard Lippert[*,†]

[†]Fakultät Chemie, Technische Unversität Dortmund, Otto-Hahn-Strasse 6, 44221 Dortmund, Germany

[‡]Departamento de Química Inorgánica, Instituto de Síntesis Química y Catálisis Homogénea (ISQCH), Universidad de Zaragoza−CSIC, 50009 Zaragoza, Spain

Supporting Information

ABSTRACT: The synthesis and characterization of three heteronuclear Pt_2Pd_2 (**4**, **5**) and $PtPd_2$ (**6**) complexes of the model nucleobase 9-methyladenine (9-MeA) is reported. The compounds were prepared by reacting $[Pt(NH_3)_3(9\text{-MeA-}N7)](ClO_4)_2$ (**1**) with $[Pd(en)(H_2O)_2](ClO_4)_2$ at different ratios *r* between Pt and Pd, with the goal to probe Pd^{II} binding to any of the three available nitrogen atoms, N1, N3, N6 or combinations thereof. Pd^{II} coordination occurs at N1 and at the deprotonated N6 positions, yet not at N3. **4** and **5** are isomers of $[\{(en)Pd\}_2\{N1,N6\text{-}9\text{-MeA}^-\text{-}N7\}Pt(NH_3)_3\}_2](ClO_4)_6\cdot nH_2O$, with a head−head orientation of the two bridging 9-MeA^- ligands in **4** and a head−tail orientation in **5**. **6** is $[\{(en)Pd\}_2(OH)(N1,N6\text{-}9\text{MeA}^-\text{-}N7)Pt(NH_3)_3](ClO_4)_4\cdot 4H_2O$, hence a condensation product between $[Pt(NH_3)_3(9\text{-MeA-}N7)]^{2+}$ and a μ-OH bridged dinuclear (en)Pd−OH−Pd(en) unit, which connects the N1 and N6 positions of 9-MeA^- in an intramolecular fashion. **4** and **5**, which slowly interconvert in aqueous solution, display distinct structural differences such as significantly different intramolecular Pd···Pd contacts (3.124 0(16) Å in **4**; 2.986 6(14) Å in **5**), among others. Binding of $(en)Pd^{II}$ to the exocyclic N6 atom in **4** and **5** is accompanied by a large movement of Pd^{II} out of the 9-MeA^- plane and a trend to a further shortening of the C6−N6 bond as compared to free 9-MeA. The packing patterns of **4** and **5** reveal substantial anion−π interactions.

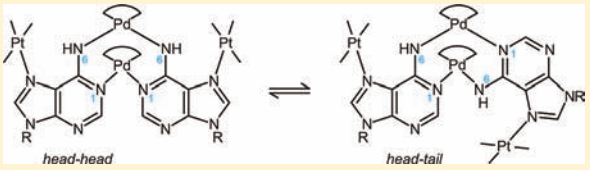

1. INTRODUCTION

Purine nucleobases (adenine, guanine, hypoxanthine) not only are constituents of DNA and RNAs but at the same time represent an important class of protein cofactors ("purinome") involved in many key cellular processes.[1] Being at the same time excellent ligands for metal ions and among the preferred ones in nucleic acids, a detailed understanding of the coordinating properties of purines is highly desirable and has in fact been the aim of numerous studies.[2] It has long been known that the N7 positions of N9 blocked purine nucleobases are kinetically favored binding sites for numerous main group and transition metal ions, including for Pt antitumor agents.[2a,b,d] On the other hand, the involvement of donor sites in the pyrimidinic entities of the purine bases is less well studied, as are multinuclear or even heteronuclear complexes of these ligands. By deliberately blocking the N7 site of a N9-substituted purine by a coordinatively saturated and inert metal entity such as $(NH_3)_3Pt^{II}$, $(dien)Pt^{II}$, or *cis*- or *trans*-$(NH_3)_2LPt^{II}$ (dien = diethylenetriamine, L = other nucleobase), the coordination properties of the pyrimidine part can be explored in more detail. Applying this approach, we have studied, for example, metal migration processes from N1 to the exocyclic N6 site in 9-methyladenine (9-MeA)[3a,b] and have prepared C_3-symmetric molecular vases with 9-alkyl-hypoxanthine (9-RHx) ligands, with $(en)Pd^{II}$ bridging N1 and N3 sites intermolecularly.[3c] The idea to synthesize an analogous vase applying the model nucleobase 9-MeA failed, however. Rather than binding to N1 and N3, as in the case of the anionic 9-alkylhypoxantinate ligands, $(en)Pd^{II}$ prefers N1 and the exocyclic amino group N6 of 9-MeA, with deprotonation of the latter (Scheme 1). As it turned out, $(en)Pd^{II}$ bridging via N1 and N6H can occur in two ways, leading to *head−head* (*hh*) and *head−tail* (*ht*) isomers. Although these two isomers can form, in principle, by different ways, it was also observed that in aqueous solution a mutual isomerization from the head−head to the head−tail isomer is possible.

2. EXPERIMENTAL SECTION

Materials and Methods. K_2PtCl_4 and adenine were of commercial origin. The following compounds were prepared as described in the literature: 9-methyladenine,[4] $Pd(en)Cl_2$,[5] and $[Pt(NH_3)_3(9\text{-MeA-}N7)](ClO_4)_2$.[6]

Characterization and NMR Measurements. Elemental (C, H, N) analysis data were obtained on a Leco CHNS-932 instrument. ^{1}H NMR spectra in D_2O were recorded on Varian Mercury 200 FT NMR, Bruker DRX 400, and/or Bruker AC 300 instruments with sodium-3-(trimethysilyl)propanesulfonate

Received: July 20, 2011
Published: September 22, 2011

Scheme 1. Different Reaction Pathways of $[Pta_3(pu-N7)]^{2+}$ with $(en)Pd^{II}$ (pu = 9-RHxH or 9-MeA)

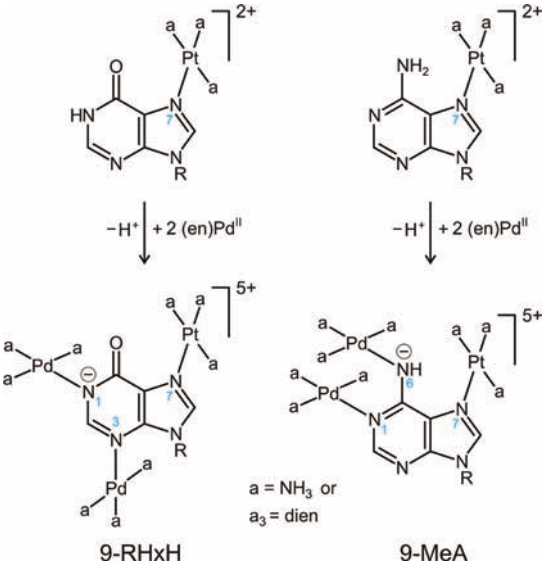

(TSP, δ = 0.0 ppm) as the internal reference. pD values of NMR samples were determined by use of a glass electrode and addition of 0.4 units to the uncorrected pH meter reading (pH*).[7] pK_a values were determined by means of pD dependent ^{1}H NMR spectroscopy, and the changes in the chemical shifts of protons resulting from changes in pD were evaluated by a nonlinear least-squares fit according to the Newton-Gauss method.[8] The pK_a values for D_2O, obtained by this method, were then converted to H_2O.[9] Mass spectra (ionization mode electrospray ionization-high-resolution mass spectrometry (ESI-HRMS)) was generated on a "LTQ Orbitrap" (Fourier transform mass spectrometer) coupled to an "Accela" high-pressure liquid chromatography (HPLC)-system.

Preparation of hh-[{(en)Pd}$_2${(N1,N6-9-MeA$^-$-N7)Pt(NH$_3$)$_3$}$_2$]-(ClO$_4$)$_6$·4H$_2$O (**4**). A suspension of Pd(en)Cl$_2$ (237.90 mg, 1 mmol) and AgClO$_4$ (415.48 mg, 2 mmol) in water (30 mL) was stirred at room temperature with daylight excluded for 24 h. After cooling (ice-bath) and filtration of AgCl, the solution was added to a suspension of $[Pt(NH_3)_3(9\text{-MeA-}N7)](ClO_4)_2$ (595.43 mg, 1 mmol) in water (20 mL), and the pH was raised to ~5.5−6.0 by means of NaOH. The reaction mixture was stirred at 40 °C for 4 h, and after filtration, concentrated by rotary evaporation to ~40−50 mL and allowed to crystallize at 4 °C. Slightly yellow crystals appeared after several days, which proved to be the *hh*-dimer by X-ray crystallography. Yield: 10% (80 mg). Elemental analysis is in agreement with the presence of six water molecules, but X-ray crystallography showed four water molecules only. Calcd (%) for $C_{16}H_{58}Cl_6N_{20}O_{30}Pt_2Pd_2$: C, 10.54; H, 3.20; N, 15.37. Found: C, 10.6; H, 3.2; N, 15.4. ^{1}H NMR (δ/D$_2$O, pD = 7.2): 8.67 (s, 1H, H8), 8.34 (s, 1H, H2), 7.07 (s, 1H, NH), 3.73 (s, 3H, CH$_3$), 3.15−2.90 (m, 4H, CH$_2$-en).

Preparation of ht-[{(en)Pd}$_2${(N1,N6-9-MeA$^-$-N7)Pt(NH$_3$)$_3$}$_2$]-(ClO$_4$)$_6$·7H$_2$O (**5**). Keeping the mother solution from which **4** had been isolated at 4 °C, after several weeks orange-yellow crystals appeared in the solution which proved to be the *ht*-dimer by X-ray crystallography. Crystals of **5** were separated by hand under a microscope. From ^{1}H NMR, the yield of **5** was estimated to be 15%. ^{1}H NMR (δ/D$_2$O, pD = 6.7): 8.80 (s, 1H, H8), 8.35 (s, 1H, H2), 6.87 (s, 1H, NH), 3.71 (s, 3H, CH$_3$), 3.11 (m, 2H, CH$_2$-en), 2.95 (m, 2H, CH$_2$-en).

Preparation of [{(en)Pd}$_2$(OH)(N1,N6-9MeA$^-$-N7)Pt(NH$_3$)$_3$]-(ClO$_4$)$_4$·4H$_2$O (**6**). A suspension of Pd(en)Cl$_2$ (237.90 mg, 1 mmol) and AgClO$_4$ (415.48 mg, 2 mmol) in water (10 mL) was stirred at room temperature with daylight excluded for 24 h. After cooling (ice-bath) and filtration of AgCl, the solution was added to a suspension of $[Pt(NH_3)_3(9\text{-MeA-}N7)](ClO_4)_2$ (148.86 mg, 0.25 mmol) in water (10 mL) and the pH raised to ~6 with NaOH. The reaction mixture was stirred at 40 °C for 4 h and, after filtration, concentrated by rotary evaporation to ~2 mL, giving a brownish solid which was recrystallized from H_2O (7 mL of H_2O at 40 °C) to give a yellowish solid. Yield: 30% (105 mg). Anal. Calcd (%) for $C_{10}H_{40}Cl_4N_{12}O_{21}PtPd_2$: C 9.91, H 3.33, N 13.88. Found: C 10.0, H 3.2, N 13.7. ^{1}H NMR (δ/D$_2$O, pD = 7.17): 8.48 (s, 1H, H8), 8.16 (s, 1H, H2), 7.32 (s, 1H, NH), 3.82 (s, 3H, CH$_3$), 2.86 (m, 8 H, CH$_2$-en). **6** was characterized by ESI-MS (see Supporting Information).

X-ray Data Collection. X-ray crystal data for **4** and **5** were collected on an Oxford Diffraction Xcalibur S diffractometer with graphite monochromated Mo Kα radiation (0.710 73 Å). Data reduction was done with the CrysAlisPro software.[10] Both structures were solved by direct methods and refined by full-matrix least-squares methods based on F^2 using the SHELXL-97 and WinGX software.[11] All non-hydrogen atoms were refined anisotropically, and all the hydrogen atoms were positioned geometrically in idealized positions and refined with isotropic displacement parameters according to the riding model. All calculations were performed using the SHELXL-97 and WinGX programs.[11] Refinement parameters for **4** and **5** are as follows.

Crystal Data for hh-[{(en)Pd}$_2${(N1,N6-9-MeA$^-$-N7)Pt(NH$_3$)$_3$}$_2$]-(ClO$_4$)$_6$·4H$_2$O (**4**). $C_{16}H_{54}Cl_6N_{20}O_{28}Pd_2Pt_2$, M = 1790.47 g mol^{-1}, slightly yellow blocks, orthorhombic, space group *Pnma*, a = 19.6292(8) Å, b = 23.5594(10) Å, c = 10.8658(5) Å, V = 5024.9(4) Å^3, Z = 4, D_{calc} = 2.367 g cm^{-3}, T = 150(2) K, with Mo Kα (λ = 0.710 73), 18 418 reflections collected, 6 110 unique (R_{int} = 0.0466), R_1 [$I > 2\sigma(I)$] = 0.0594, wR_2 (F, all data) = 0.1655, GoF = 0.976. CCDC 831339.

Crystal Data for ht-[{(en)Pd}$_2${(N1,N6-9-MeA$^-$-N7)Pt(NH$_3$)$_3$}$_2$]-(ClO$_4$)$_6$·7H$_2$O (**5**). $C_{16}H_{60}Cl_6N_{20}O_{31}Pd_2Pt_2$, M = 1844.52 g mol^{-1}, orange blocks, monoclinic, space group $P2_1/c$, a = 13.9122(9) Å, b = 18.0415(6) Å, c = 22.1210(10) Å, β = 105.688(6)°, V = 5345.5(5) Å^3, Z = 4, D_{calc} = 2.292 g cm^{-3}, T = 150(2) K, with Mo Kα (λ = 0.710 73), 75 049 reflections collected, 12 117 unique (R_{int} = 0.0562), R_1 [$I > 2\sigma(I)$] = 0.0796, wR_2 (F, all data) = 0.1661, GoF = 1.026. CCDC 831340.

3. RESULTS AND DISCUSSION

^{1}H NMR Scale Reactions. $[Pt(NH_3)_3(9\text{-MeA-}N7)](ClO_4)_2$ (**1**), prepared as reported before,[6] was reacted with $[Pd(en)(D_2O)_2]^{2+}$ in D_2O at different ratios r, and the reactions were followed by ^{1}H NMR spectroscopy. pD values were typically in the range 4−6, depending on r. Figure 1 displays the ^{1}H NMR spectrum of a sample with r(Pt/Pd) = 1:0.5. Relative intensities of the various species present in solution and, in part, the number of the resonances were dependent on r and pD. The assignment made in Figure 1 was based on comparison with authentic samples isolated on a preparative scale (**1**, **4**, **5**) or is tentative only (**2**, **3**). In no instance was coordination of $(en)Pd^{II}$ to N3 of 9-MeA observed, as this binding pattern should have led to a characteristic downfield shift of the CH$_3$(N9) resonance, as

dx.doi.org/10.1021/ic201548k |*Inorg. Chem.* 2011, 50, 10439–10447

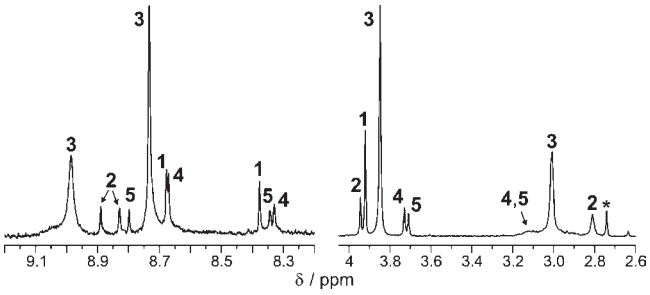

Figure 1. ^{1}H NMR spectrum (300 MHz) of a mixture of **1** and $[Pd(en)(D_2O)_2]^{2+}$ (2:1) in D_2O after 4 h at 40 °C, with pD being 4.1. Five different species can be differentiated. The intensity of the downfield part of the spectrum is increased for clearness. ∗ indicates free $[(en)Pd(D_2O)]^{2+}$.

previously demonstrated.[3c,12] Altogether five sets of adenine resonances are observed. The differentiation of aromatic H2 and H8 resonances was accomplished in several instances by 1D nuclear Overhauser effect (NOE) spectra, relying on the spatial proximity of H8 and CH_3 resonances (Supporting Information). Resonances due to the starting compound **1** were identified by their pD dependence (Supporting Information). The two minor resonances at 8.89 and 8.83 ppm are assigned to the PtPd complex $[(en)(D_2O)Pd(N1\text{-}9\text{-}MeA\text{-}N7)Pt(NH_3)_3]^{4+}$ (**2**). Both aromatic 9-MeA resonances of **2** are downfield relative to those of the starting compound **1**, consistent with metals bonded at N7 and N1. Moreover, both resonances are sensitive to Cl^-, in agreement with the presence of an exchangeable water ligand. Thus, addition of NaCl to an acidic solution of **2**, or incomplete removal of Cl^- from $Pd(en)Cl_2$ by $AgNO_3/AgClO_4$, shifts the resonances slightly upfield, to 8.82 and 8.80 ppm for $[(en)ClPd(N1\text{-}9\text{-}MeA\text{-}N7)Pt(NH_3)_3]^{3+}$.

The most intense resonances are those of the Pt_2Pd complex $[(en)Pd\{(N1\text{-}9\text{-}MeA\text{-}N7)Pt(NH_3)_3\}_2]^{6+}$ (**3**). This assignment is consistent with the relative intensities of the CH_3 resonance (3.85 ppm) and the CH_2 signals of the en ligand (3.01 ppm), the expected downfield shifts of H2 and H8 in N1,N7 dimetalated 9-MeA relative to those in **1**, as well as comparison with the NMR spectrum of the X-ray structurally characterized Pt_3 analogue.[13] The relative broadness of the H2 resonance at 8.99 ppm suggests rotation of the $Pt(NH_3)_3$(9-MeA-*N7*) entity about the Pd−N1 bonds in **3**.

The two remaining sets of adenine resonances are assigned to tetranuclear Pt_2Pd_2 species, $[\{(en)Pd\}_2\{(N1,N6\text{-}9\text{-}MeA^-\text{-}N7)\text{-}Pt(NH_3)_3\}_2]^{6+}$ in their head−head (**4**) and head−tail (**5**) isomer forms. Both complexes were isolated and characterized by X-ray crystallography (see below). Relative yields of these Pt_2Pd_2 complexes become larger as the ratio *r* between **1** and $(en)Pd^{II}$ decreases and the pH is moderately raised (∼6). For example, with $r = 1$, essentially three species are observed in solution with relative intensities being **4** > **5** ≫ **1**. With a larger excess of $(en)Pd^{II}$ over **1** ($r \leq 0.5$), yet another complex **6** is formed, which will likewise be discussed separately. Its formation is not observed under the conditions applied in Figure 1. The chemical shifts of all resonances of **1**−**6** are provided in the Supporting Information.

Scheme 2 lists possible pathways to the various species observed in the ^{1}H NMR spectra (see, e.g., Figure 1). Initial binding of $(en)Pd^{II}$ to the available unprotonated N1 position is assumed, whereas N3 binding is to be excluded. While formation of **2** and **3** is straightforward, reaction pathways to the Pt_2Pd_2 complexes **4** and **5** are variable, with at least several feasible intermediates (**2a**, **3a**, **3b**) resulting from migration processes of $(en)Pd^{II}$ from N1 to N6 sites. Although the ^{1}H NMR spectra do not provide any evidence for the existence of such intermediates in measurable quantities, we note that with $(en)Pd^{II}$ replaced by *cis*-$(NH_3)_2Pt^{II}$, analogues of **3a** and **3b** have been isolated at basic pH.[3b]

Head−Head-Pt_2Pd_2 Complex 4. Figure 2 gives a view of the cation *hh*-$[\{(en)Pd\}_2\{(N1,N6\text{-}9\text{-}MeA^-\text{-}N7)Pt(NH_3)_3\}_2](ClO_4)_6\cdot 4H_2O$ (**4**). Two $(en)Pd^{II}$ entities bridge N1 and deprotonated N6H sites of the 9-methyladeninato ligands in a head−head fashion. Salient structural features are listed in Table 1. The cation of **4** is bisected by a symmetry plane, which includes both Pd atoms (in Figure 2 it is perpendicular to the paper plane). The chelating en groups are disordered, adopting δ and λ puckers. Distances and angles around the metal centers are within the expected limits. The dihedral angle between both palladium coordination planes is 44.6(3)°, with a torsion angle of 4.6(4)° (N1−Pd1−Pd2−N6). Distances between metal centers are 3.1240(16) Å for Pd1−Pd2, and 7.2843(9) Å for both symmetry related platinum atoms. Pt1−Pd1 and Pt1−Pd2 distances are 6.5268(11) and 5.0070(9), respectively. Both adenine rings are disposed in a roof-like fashion, with an inclination of 78.4(2)°. This angle differs from the coordination N1−Pd1−N1′ and N6−Pd2−N6′ angles, 88.8(6)° and 94.6(5)°, respectively. This situation is in agreement with minor deviations involving dihedral angles and coplanarity of metals and adenines: (i) Pd1, Pd2, and N6 are located out of the adenine planes by 0.200(12) Å, 0.570(15) Å, and 0.143(13) Å, respectively. Conversely, the N1 atoms, also involved in metal coordination, are practically coplanar with the adenine ring (0.016(9) Å). (ii) The Pd2 square planar coordination plane ($Pd2N_4$) is twisted 64.3(7)° with respect to the nucleobase ring, far from the nearly right angles displayed by $Pt1N_4$ (85.9(2)°) and $Pd1N_4$ (84.2(5)°). (iii) $Pt1N_4$ displays a shorter angle with $Pd2N_4$ (67.3(6)°) than with $Pd1N_4$ (85.5(5)°). Thus, deviations occur involving the Pd2 and N6 atoms, which might be attributed to the electronic flexibility of the exocyclic N6 amino group in comparison to the endocyclic N1 atom. A related Pt_3 complex,[13] with *cis*-$(NH_3)_2Pt^{II}$ bridging the N1 sites and $(NH_3)_3Pt^{II}$ blocking both N7 positions, does not include metal coordination at N6. Consequently, the geometry and arrangement of this molecule differs from **4**, as evidenced by the different distances between both N6 sites: 3.35 Å in the Pt_3 compound and 2.969(17) Å in **4**. Distances between both coordinated N1 sites are similar, namely, 2.93 and 2.84(2) Å, respectively.

The only other example of a dinuclear metal complex with head−head arranged adenine ligands bridging the N1 and N6 sites is a dirhenium(III) complex.[14] The quadruple bond between the two metals in this compound leads to a very short Re−Re distance of 2.2455(10) Å.

The disposition of cation **4** fits perfectly for host−guest interactions with the perchlorate counteranions. As shown in Figure 3, a ClO_4^- anion is inserted between the adenine rings of the cation and stabilized via the following combination of interactions: (i) electrostatic attraction between the +6 charged cation **4** and the ClO_4^- anion; (ii) hydrogen bonding, with a 2-fold interaction between N11(H_3)···O12 (2.951(13) Å), and (iii) anion−π interactions between O11 and the pyrimidinic ring of the adenine (distance to both centroids, 3.02 Å) and between O13 and the imidazolic ring (distance to both centroids, 3.26 Å).

dx.doi.org/10.1021/ic201548k |*Inorg. Chem.* 2011, 50, 10439–10447

Scheme 2. Possible Pathways to the Formation of 2, 3, 4, and 5[a]

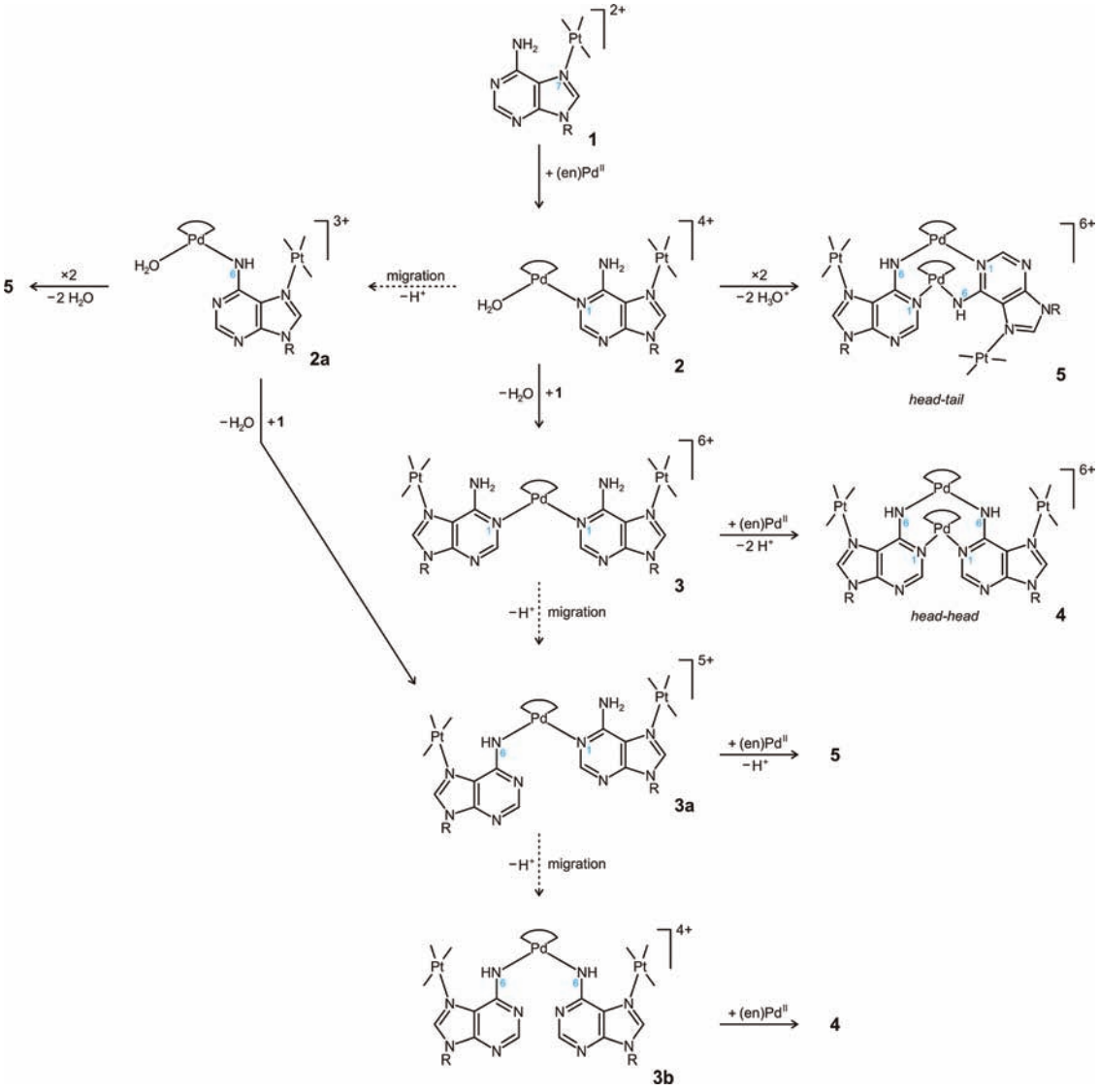

[a] Many of the species may exist in equilibria (not indicated).

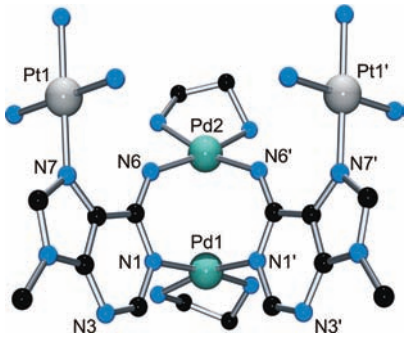

Figure 2. View of cation **4** with partial atom numbering scheme.

Table 1. Selected Bond Distances [Å] and Angles [deg] for Compound 4[a]

Pt1−N7	1.994(9)	N1−Pd1−N1′	88.8(6)°
Pd1−N1	2.028(10)	N6−Pd2−N6′	94.6(5)°
Pd2−N6	2.020(9)	Pd1N$_4$/Pd2N$_4$	44.6(3)°
C6−N6	1.281(12)	Pt1N$_4$/Ad	85.9(2)°
Pd1−Pd2	3.1240(16)	Pd1N$_4$/Ad	84.2(5)°
Pt1−Pd1	6.5268(11)	Pd2N$_4$/Ad	64.3(7)°
Pt1−Pd2	5.0070(9)	Pt1N$_4$/Pd1N$_4$	85.5(5)°
Pt1−Pt1′	7.2843(9)	Pt1N$_4$/Pd2N$_4$	67.3(6)°
C6−N6−Pd2	135.7(7)	Ad/Ad′	78.4(2)°

[a] Pt1N$_4$, Pd1N$_4$, Pd1N$_4$ platinum (palladium) coordination planes; Ad = plane defined by adenine rings. Symmetry (′) operation: x, 1.5 − y, z.

This combination of favorable interactions has been demonstrated in numerous instances to result in successful anion complexation in cationic guest systems.[15] In addition, both perchlorate O13 atoms are also involved in hydrogen bonding with the NH$_2$ sites of an en group of a neighboring cation:

dx.doi.org/10.1021/ic201548k |*Inorg. Chem.* 2011, 50, 10439–10447

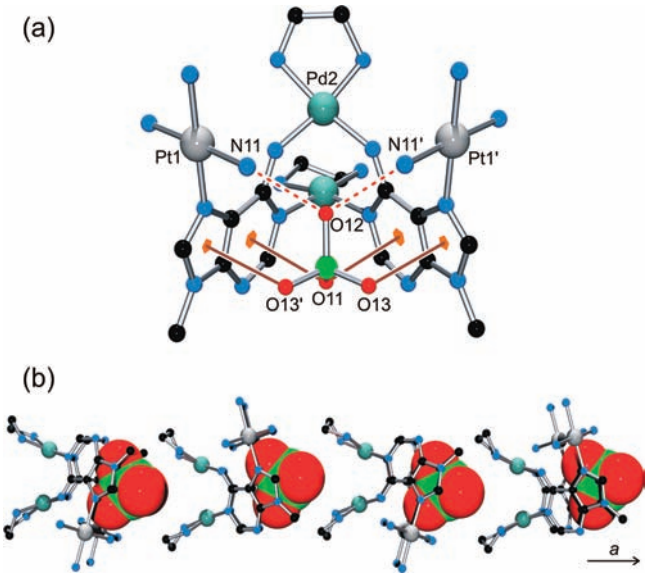

Figure 3. (a) View of host−guest interactions of cation **4** with ClO_4^-. (b) Disposition of cations of **4** and perchlorates along the *a* axis. Hydrogen atoms have been omitted.

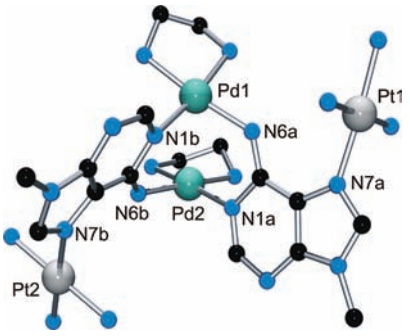

Figure 4. View of cation **5** with atom numbering scheme.

N17(H_2)···O13, 3.05(4) Å. Thus, ClO_4^- is embedded between two cations of **4**, and each cation interacts with two ClO_4^- anions, resulting in chains along the crystallographic *a* axis, with cations alternatively oriented (Figure 3b).

Head−Tail-Pt_2Pd_2 Complex 5. The cation of *ht*-[{(en)Pd}$_2$-{(*N*1,*N*6-9-MeA$^-$-*N*7)Pt(NH_3)$_3$}$_2$](ClO_4)$_6$·7H_2O (**5**) is depicted in Figure 4. As a consequence of this head−tail arrangement, the cation of **5** is inherently chiral. Both enantiomers occur in the unit cell. Structural details are given in Table 2. Both halves of **5** display significant differences when compared to each other in the solid state structure. The roof-like conformation as seen in **4** is maintained, with opposite (head−tail) orientation of the Pt(NH_3)$_3$(9-MeA) fragments. In cation **5**, the dihedral angle between both adenines (86.6(3)°) and the N1a−Pd2−N6b (91.3(5)°), and N6a−Pd1-N1b (94.2(5)°) angles are closer to 90°, in comparison to cation **4**. Dihedral angles between PtN_4 and their corresponding adenine planes are 89.4(3)° and 84.0(5)° for Pt1 and Pt2, respectively. The PdN_4 coordination planes form the following angles with the adenine rings: $Pd1N_4/Ad_{(A)}$, 54.9(4)°; $Pd1N_4/Ad_{(B)}$, 86.6(3)°; $Pd2N_4/Ad_{(A)}$, 79.6(4)°; $Pd2N_4/Ad_{(B)}$, 66.5(3)°, again with remarkable deviations about the Pd−N6 bonds. The two $Pd1N_4$ and $Pd2N_4$ planes form a dihedral angle of 36.7(3)°, with torsion angle values more pronounced than in **4**: N6a−Pd1−Pd2−N1a, 20.8(5)°; N1b−Pd1−Pd2−N6b, 16.8(5)°. The Pd1−Pd2 distance is 2.9866(14) Å, significantly shorter than in **4**, and a direct consequence of the larger torsion angle in **5**.[16] The distance between both platinum atoms displays an obviously longer value, 10.0239(8) Å. Concerning heterometallic Pt−Pd distances, those involving Pt2 (Pt2−Pd2, 5.0247(14) Å and Pt2−Pd1, 6.5273(12) Å) are almost identical with those in complex **4** (cf. Table 1: 5.0070(9) Å, 6.5268(11) Å), whereas the Pt1−Pd1 (5.1210(11) Å) and Pt1−Pd2 (6.3918(12) Å) distances clearly differ from these values. When comparing both halves of complex **5**, there are some critical differences relating to the adenine bases and more specifically involving the N6 sites. In the case of adenine B, similar values as in cation **4** are observed, relating distances to the $Ad_{(B)}$ plane from Pt2, 0.054(15) Å; Pd1, −0.337(14) Å; Pd2, 0.388(18) Å; N6b, −0.007(17) Å. The geometry of the $Ad_{(A)}$-half displays noteworthy differences, with longer distances to the $Ad_{(A)}$ plane from Pt1, 0.230(16) Å; Pd1, −0.76(2) Å; Pd2, 0.475(14) Å; and N6a, −0.214(19) Å.

A related Pt_2 complex, with two *cis*-$(Me_3P)_2Pt^{II}$ units bridging the N1 and N6 sites, displays a basic structural analogy with **5** but shows some peculiarities such as longer Pt−P distances (avg 2.26 Å), steric hindrance of the phosphine groups resulting in wider Pt−N1−N6−Pt torsion angles of 30.6° (avg), almost coplanarity of both N6 atoms with the adenine rings, and longer distances

Table 2. Selected Bond Distances [Å] and Angles [deg] for Compound 5[a]

Pt1−N7a	2.012(11)	Pt1−Pt2	10.0239(8)°
Pt2−N7b	2.016(13)	N1a−Pd2−N6b	91.3(5)°
Pd1−N6a	2.007(11)	N6a−Pd1−N1b	94.2(5)°
Pd1−N1b	2.022(12)	C6a−N6a−Pd1	130.3(9)°
Pd2−N6b	1.970(12)	C6b−N6b−Pd2	128.7(9)°
Pd2−N1a	2.041(12)	$Pd1N_4/Pd2N_4$	36.7(3)°
C6a−N6a	1.309(17)	$Pt1N_4/Ad_{(A)}$	89.4(3)°
C6b−N6b	1.297(18)	$Pt2N4/Ad_{(B)}$	84.0(5)°
Pd1−Pd2	2.9866(14)	$Pd1N_4/Ad_{(A)}$	54.9(4)°
Pt1−Pd1	5.1210(11)	$Pd1N_4/Ad_{(B)}$	86.6(3)°
Pt2−Pd2	5.0247(14)	$Pd2N_4/Ad_{(A)}$	79.6(4)°
Pt1−Pd2	6.3918(12)	$Pd2N_4/Ad_{(B)}$	66.5(3)°
Pt2−Pd1	6.5273(12)	$Ad(A)/Ad_{(B)}$	86.6(3)°

[a] $Pt1N_4$, $Pt2N_4$, $Pd1N_4$, $Pd2N_4$ platinum (palladium) coordination planes; $Ad_{(A)}$, $Ad_{(B)}$ = plane defined by adenine A (or B) rings.

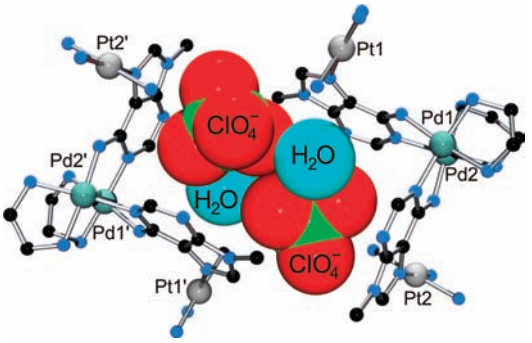

Figure 5. View of the two trapped perchlorate anions and two water molecules between pairs of cations **5**.

from N1- than from N6-coordinated Pt atoms to the adenine rings.[17]

The wider lateral cavity of cation **5** in comparison to **4** allows for accommodation of a perchlorate counteranion and a water molecule. Both guest molecules are connected to each other via hydrogen bonding (O3w···O12, 3.01(2) Å), but only the water molecule interacts with the cation in this way (O3w···N11, 2.890(19) Å). The perchlorate anion interacts with cation **5** by electrostatics and three additional anion−π interactions: with both $Ad_{(B)}$-rings, distances from O11 and O13 to the ring centroids are 3.17 and 3.11 Å, respectively, and the imidazolic ring of $Ad_{(A)}$ (O11-centroid, 3.24 Å). In addition, a second hydrogen bond of O12 binds a symmetry related O3w water molecule (2.97(2) Å), thus encapsulating two perchlorate anions and two water molecules in the cavity formed by a pair of cations of **5** (Figure 5 and Supporting Information). This situation is reminiscent of the behavior of *cis*-$[Pt(NH_3)_2(9\text{-MeAH-}N7)_2]^{4+}$, which forms rectangular channels with stacked nitrate anions inside.[18]

The C6−N6 Bond of Adenine in 4 and 5. The C6−N6 bond length in 9-MeA (1.329(2) Å[19]) as well as in a series of related adenine ligands (1.337(2) Å[20]) is consistent with a substantial degree of double bond character, as is the (essentially) sp^2 hybridization state of the N atom in the amino group $N6H_2$.[21] As expected, protonation of the N1 site causes a slight shortening of this bond (1.322(3) Å[20]). Both in **4** and in **5** this bond shows a trend to even shorter distances, which at least with **4** (1.282(12) Å) and in comparison with neutral adenine ligands, is significant.[22] This trend also holds up for a Pt^{II} complex with Pt^{II} bonded to both N7 and N6 in anionic 9-methyladeninato ligands (1.296(7) Å[2b]). With N6 platinated neutral adenine ligands (hence protonated at N1 and therefore, formally, a metalated form of a rare adenine tautomer[23]) the situation is ambiguous (1.280(14) Å[23b]), but as N1 is protonated, the situation is different from that in **4** and **5**. Our findings thus suggest that deprotonation of the exocyclic amino group of 9-MeA and metal coordination to both N1, N6, and N7 causes strengthening of the C6−N6 double bond character. This situation consequently contrasts with that seen in 1-methylcytosinate, where metal coordination to the deprotonated $N4H^-$ group as well as to N3 can go along with a lengthening of the C4−N4 bond and a shift toward sp^3 hybridization of N4.[24] What is striking, both in **4** and **5**, are the substantial deviations of the Pd atoms bonded to N1 and N6 from the adenine planes (see above). They appear to be, at least in part, considerably larger than in mononuclear transition metal−nucleobase complexes and may in the cases of **4** and **5** be a consequence of the distortions caused by dimer formation via N1 and N6. However, it may be also facilitated by changes in the electronic structure of the 3-fold metalated adenine, e.g., a change in N6 hybridization, and an involvement of the π-electrons of C6−N6 in metal binding.[25] Interestingly, in the dirhenium(III) complex mentioned above,[14] the N6 atom appears to retain its sp^2 hybridization state, as judged from the C6−N6 distance (1.346(16) Å) and the C6−N6−Re angle of 123.8(9)°.

^{1}H NMR Spectra of 4 and 5. ^{1}H NMR spectra of **4** and **5** in D_2O are given in Figure 6. The assignment of H8 (8.67 ppm) and H2 (8.34 ppm) resonances of the adenine ligands of **4** is based on 1D NOE experiments. Interestingly the NH proton of the exocyclic N6H group exchanges only slowly with deuterium and is detectable at 7.07 ppm for a while. The methylene protons of the two en ligands occur as three sets of multiplets between

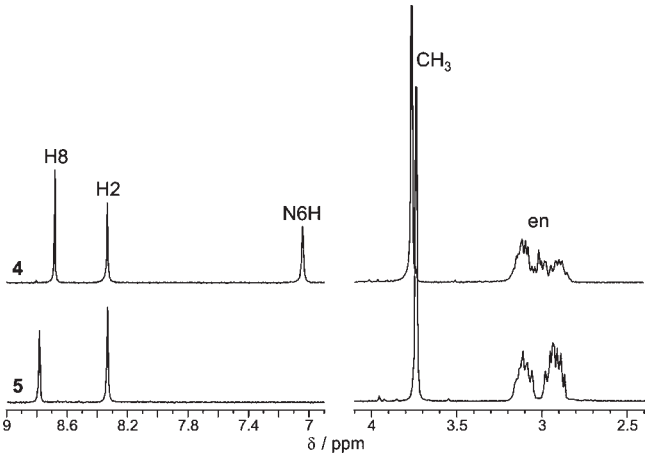

Figure 6. ^{1}H NMR (D_2O, pD ∼ 6) spectra of compounds **4** (top) and **5** (bottom). One CH_2 group of TSP used as internal reference is superimposed with CH_2 of the en ligand in **5**.

2.90 and 3.15 ppm. Resonances of the head−tail isomer **5** are similar to those of **4**, with N6H likewise detected at 6.87 ppm, albeit in freshly prepared solutions only. The CH_2 protons of the en ligands are observed as two multiplets, centered around 2.9−3.1 ppm. Features of the en resonances in **4** and **5** contrast those seen in simple complexes such as $[Pd(en)(D_2O)_2]^{2+}$ or $[Pd(en)L_2]^{2+}$ (L = N-heterocyclic ligands), where they form somewhat broadened singlets. We assume that this difference is a consequence of a slowing down of interconversion of the chelate rings ($\delta \rightleftharpoons \lambda$) due to steric interference between the two adjacent ligands. A similar observation can be made with the head−tail isomer of $[Pt(en)(1\text{-MeC}^-\text{-}N3,N4)]_2^{2+}$ (1-MeC$^-$ = 1-methylcytosine, deprotonated at N4).[26]

Isomerization Reactions of 4 and 5. The ^{1}H NMR spectra of individual samples of **4** and **5** in D_2O (pD ≃ 6; samples kept at 40 °C) change with time, revealing the gradual formation of the respective other isomer. These reactions are slow, with half-life times on the order of 70 days (Figure 7 and Supporting Information). As the aromatic protons of the adeninato ligands undergo isotopic exchange,[27] reactions are best followed by monitoring the CH_3 resonances: (i) The isomerization reaction **4** → **5**, hence the conversion of the *hh* isomer into the *ht* isomer, is accompanied by the gradual appearance of a resonance of low intensity (6% after 80 days) of the starting compound **1** as well as another resonance of lower intensity centered at 3.8 ppm which cannot be assigned. The small amount (<4%) of the *ht* isomer observed immediately after sample preparation is attributed to an impurity of **5** in **4** rather than to rapid formation of **5** from **4**. (ii) A freshly prepared solution of the *ht* isomer **5** reveals no *hh* isomer **4** to be present, yet a small fraction of about 1−2% of **1**, which remains constant throughout the reaction time of 80 days.

Reversible isomerization reactions between *hh* and *ht* diplatinum(II)[28] and dipalladium(II) complexes[29] containing α-pyridonato ligands have been reported before. They take place considerably faster, presumably as a consequence of the weaker M−O bonds as compared to the Pd−N6 bonds in **4** and **5**, with half-lifes of ∼7 and 0.5 h, respectively. For the mutual *hh* ⇌ *ht* isomerization reactions of $[Pt(en)(\alpha\text{-pyridonate})]_2^{2+}$, intramolecular mechanisms with cleavage of one of the two bridges have been proposed,[28] whereas such processes have been excluded in the case of the corresponding $[Pd(en)(\alpha\text{-pyridonate})]_2^{2+}$

dx.doi.org/10.1021/ic201548k |*Inorg. Chem.* 2011, 50, 10439–10447

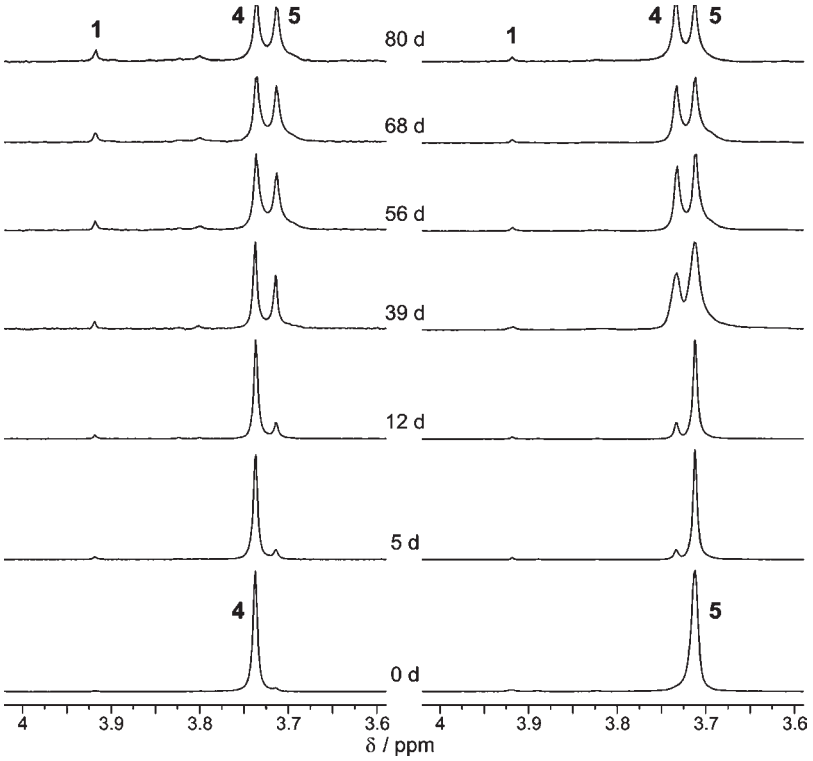

Figure 7. ^{1}H NMR spectra (D_2O, pD ≃ 6) of solutions of compounds **4** (left) and **5** (right) showing the time course of the isomerization reaction at 40 °C.

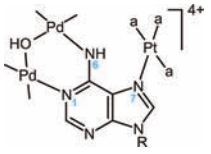

Figure 8. Proposed structure of cation **6**.

dimers.[29] Rather, in the Pd(II) system, mononuclear species have been identified in aqueous solution, suggesting that there is no "direct isomerization path" between these *hh* and *ht* Pd(II) dimers.[29] This picture is consistent with the general higher lability of Pd(II) over Pt(II) species and the ready equilibration of Pd—nucleobase complexes in solution.[30] Given the various species present in solution when **1** and $[Pd(en)(D_2O)_2]^{2+}$ are mixed (cf. Figure 1) and given the numerous pathways by which **4** and **5** can be formed (cf. Scheme 2), several of which are pH dependent, it is not possible to postulate isomerization routes. However, at least for the conversion of the *hh* isomer **4** to the *ht* isomer **5**, the ^{1}H NMR spectra suggest that an intramolecular mechanism is unlikely.

Complex 6. In the course of the ^{1}H NMR scale reactions between **1** and $[Pd(en)(D_2O)_2]^{2+}$, when **4** and **5** are formed preferentially, also formation of an additional minor species **6** was observed. **6** became the dominant species when $[Pd(en)(D_2O)_2]^{2+}$ was present in excess (e.g., **1**/Pd = 1:4, pD ≃ 6) and could be also isolated on a preparative scale. According to elemental analysis data, mass spectrometry, and relative intensities of the ^{1}H NMR resonances, **6** is assigned to a trinuclear $PtPd_2$ complex of composition $[\{(en)Pd\}_2(OH)(N1,N6\text{-}9MeA^-\text{-}N7)Pt(NH_3)_3](ClO_4)_4\cdot 4H_2O$ (Figure 8).

With the use of gentle conditions for the ionization parameters as described in the Supporting Information, it was possible to generate mass spectra of **6** containing the monocharged ion $[\mathbf{6} - 2H_2 - ClO_4^-]^+$ at m/z_{exp} = 1080 as the base peak, through the loss of one perchlorate (ClO_4^-) anion together with the loss of two molecules of hydrogen (one per $(en)Pd^{II}$ present in the complex). In addition, other ions are formed through the loss of one more or two ClO_4^- anions, yielding the 2+ and 3+ states, respectively, (m/z_{exp} = 490 for $[\mathbf{6} - 2H_2 - 2ClO_4^-]^{2+}$ and m/z_{exp} = 294 for $[\mathbf{6} - 2H_2 - 3ClO_4^-]^{3+}$). Loss of $HClO_4$ can be observed as well for the latter ions, yielding the $[\mathbf{6} - 2H_2 - ClO_4^- - HClO_4]^+$, $[\mathbf{6} - 2H_2 - 2ClO_4^- - HClO_4]^{2+}$, and $[\mathbf{6} - 2H_2 - 3ClO_4^- - HClO_4]^{3+}$, respectively (see the Supporting Information). Dehydrogenation of ethylenediamine ligands in metal complexes has been observed before,[31,32] and the mechanism for this consecutive loss of molecular hydrogen has been discussed[32a] as well as the loss of a proton accompanied with a counterion (HNO_3 in case of ref 32a). Finally, a low intensity signal also appears for the starting complex **1** as a doubly charged ion due to the loss of the two ClO_4^- anions (m/z_{exp} = 198).

In the ^{1}H NMR spectrum (D_2O, pD ≃ 7), resonances of **6** occur at 8.48 ppm (H8), 8.16 ppm (H2), 3.82 ppm (CH_3), and 2.84 ppm (CH_2-en). The N6H proton exchanges only slowly with deuterium and is observed for some time at 7.32 ppm (Supporting Information). Addition of acid (DNO_3, pD 2) to an aqueous solution of **6** causes decomposition. The major products formed are, according to ^{1}H NMR spectroscopy, complex **2** (cf. Scheme 2) and free $[Pd(en)(D_2O)_2]^{2+}$. Among the minor decomposition products, compound **3** was identified. Formation of **6** can conceivably take place via different routes (Scheme 3, top): (i) A μ-OH dipalladium(II) species, precursor of the dihydroxo-bridged dimer,[33] could bind to N1 of the 9-MeA

dx.doi.org/10.1021/ic201548k |*Inorg. Chem.* 2011, 50, 10439–10447

Scheme 3. Possible Routes from 1 to 6 (Top) and Decomposition of 6 in Acidic Medium (Bottom)

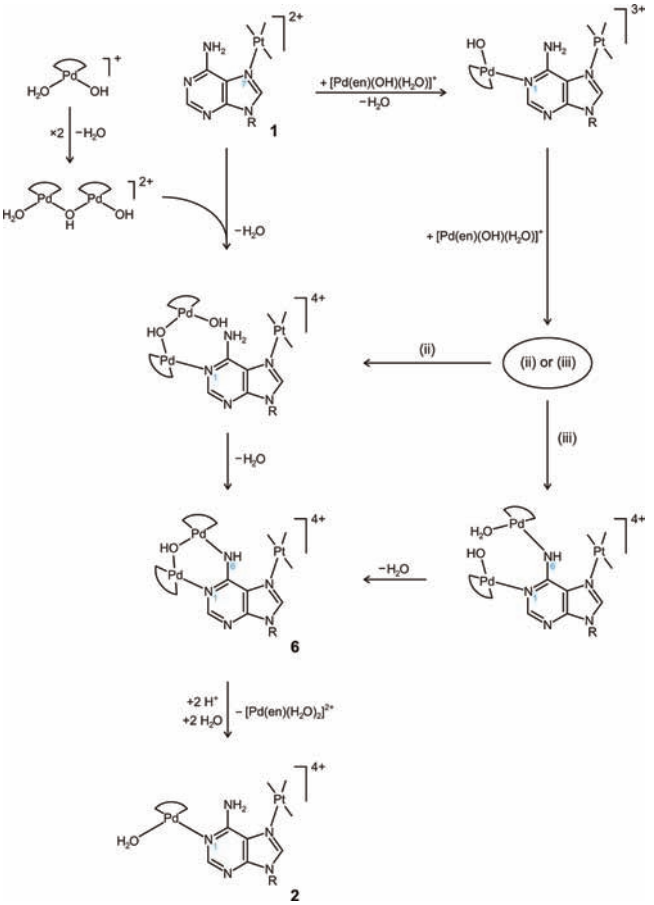

ligand in **1** and subsequently condense through its other end with $N6H_2$ of the adenine ligand. (ii) Alternatively, a monomeric $(en)Pd^{II}$ moiety could bind to N1 and subsequently condense with a second $(en)Pd^{II}$ to give a $(\mu\text{-}OH)Pd_2^{II}$ complex, which undergoes yet another condensation reaction with $N6H_2$. (iii) Finally, successive bindings of mononuclear $(en)Pd^{II}$ moieties to N1 and N6 could occur, followed by a condensation reaction leading to the OH-bridge. For a mixed Pt,Pd complex with 1-methylcytosine, carrying Pt at N3 and Pd at N4, we could recently demonstrate that pathways ii or iii are followed.[24] Realization of nucleobase complexes containing $(\mu\text{-}OH)M_2^{II}$ entities (M = Pt, Pd or Pt/Pd) is rare and has only been observed thus far with 1-methylcytosine complexes[24,34] but is more common with anionic pyrazole, triazole, and tetrazole ligands.[35]

CONCLUSIONS

In this report, we have studied heteronuclear Pt,Pd complexes of the model nucleobase 9-MeA. Blockage of the N7 position of 9-MeA by an inert $(NH_3)_3Pt^{II}$ unit and subsequent reaction of the $[Pt(NH_3)_3(9\text{-MeA-}N7)]^{2+}$ cation **1** with additional $(en)Pd^{II}$ cations leads to multinuclear species (PtPd (**2**), Pt_2Pd (**3**), Pt_2Pd_2 (**4**, **5**), and $PtPd_2$ (**6**)), in which Pd cross-linking via N1 and N6 positions of the adenine nucleobase occurs either in an intermolecular fashion (**1**, **3**, **4**, **5**) or in an intramolecular fashion (**6**). Binding of $(en)Pd^{II}$ to the N3 position of the adenine nucleobase is not observed under the conditions applied, even though simultaneous N1 and N7 metal binding does not exclude additional metal coordination to N3 *per se*.[36] Neither is the formation of a metallatriangle via N1 and N6 observed,[37] as the $(NH_3)_3Pt^{II}$ moiety at N7 does not permit an $(en)Pd^{II}$ entity at N6 to adopt an anti orientation (with respect to the $(en)Pd^{II}$ at N1) required for the formation of such a species. Our findings add to a more comprehensive understanding of formation processes (e.g., of **6**) and isomerization reactions (e.g., **4** and **5**) of metal complexes of 9-MeA, even though mechanistic details of these are still fragmentary. Also, a comprehensive understanding of the effects of multiple metal binding to 9-MeA on the behavior of the exocyclic amino group (e.g., bonding situation at N6 and hybridization of N; proper description of C6−N6 bond order) remains a challenge for the future.

ASSOCIATED CONTENT

Supporting Information. Additional spectroscopic, NMR, and ESI-MS information. This material is available free of charge via the Internet at http://pubs.acs.org.

AUTHOR INFORMATION

Corresponding Author

*E-mail: pablo.sanz@unizar.es (P.J.S.M.). Fax, (+49)231-755-3797; e-mail, bernhard.lippert@tu-dortmund.de (B.L.).

Author Contributions

§S.I. and F.M.A. have contributed equally to these results.

ACKNOWLEDGMENT

This work was supported by the Deutsche Forschungsgemeinschaft, the Fonds der Chemischen Industrie and the TU Dortmund. P.J.S.M. thanks the Spanish Ministry of Science and Innovation for funding through the "Ramón y Cajal" program. S.I. thanks the Spanish Ministry of Science and Innovation for a postdoctoral fellowship. Andreas Brockmeyer and Chantale Sevenich (TU Dortmund) are kindly acknowledged for their help with the ESI-MS analysis.

REFERENCES

(1) Hagstead, T. A. J. *Curr. Top. Med. Chem.* **2006**, *6*, 1117–1127.

(2) See, e.g., (a) various articles in *Nucleic Acid-Metal Ion Interactions*; Hud, N. V., Ed.; Royal Society of Chemistry; Cambridge, U.K., 2009. (b) Various articles in *Metal Complex-DNA Interactions*; Hadjiliadis, N., Sletten, E.; Eds.; Wiley: Chichester, U.K., 2009. (c) Houlton, A. *Adv. Inorg. Chem.* **2002**, *53*, 87–158.(d) Bau, R.; Sabat, M. In *Cisplatin. Chemistry and Biochemistry of a Leading Anticancer Drug*; Lippert, B., Ed. VHCA Zürich and Wiley-VCH: Weinheim, Germany, 1999. (e) Marzilli, L. G.; Kistenmacher, T. J.; Eichhorn, G. In *Nucleic Acid−Metal Ion Interactions*; Spiro, T. G., Ed.; Wiley: New York, 1980. (f) Various articles in *Metal Ions in Biological Systems*; Sigel, H., Ed.; Marcel Dekker: New York, 1979; Vol. 8.

(3) (a) Garijo Añorbe, M.; Lüth, M. S.; Roitzsch, M.; Morell Cerdà, M.; Lax, P.; Kampf, G.; Sigel, H.; Lippert, B. *Chem.—Eur. J.* **2004**, *10*, 1046–1057. (b) Garijo Añorbe, M.; Welzel, T.; Lippert, B. *Inorg. Chem.* **2007**, *46*, 8222–8227.(c) Ibañez, S.; Alberti, F. M.; Sanz Miguel, P. J.; Lippert, B. *Chem. Eur. J.* **2011**, *17*, 9283–9287.

(4) Talman, E. G.; Brüning, W.; Reedijk, J.; Spek, A. L.; Veldman, N. *Inorg. Chem.* **1997**, *36*, 854–861.

(5) McCormick, B. J.; Jaynes, E. N., Jr.; Kaplan, R. I. *Inorg. Synth.* **1972**, *13*, 216–217.

(6) Beyerle-Pfnür, R.; Jaworski, S.; Lippert, B.; Schöllhorn, H.; Thewalt, U. *Inorg. Chim. Acta* **1985**, *107*, 217–222.
(7) Lumry, R.; Smith, E. L.; Glantz, R. R. *J. Am. Chem. Soc.* **1951**, *73*, 4330–4340.
(8) Tribolet, R.; Sigel, H. *Eur. J. Biochem.* **1987**, *163*, 353–363.
(9) Martin, R. B. *Science* **1963**, *139*, 1198–1203.
(10) Oxford Diffraction (Poland). *CrysAlisPro*; 2010.
(11) (a) Sheldrick, G. M. *SHELXS97 and SHELXL97*; University of Göttingen: Göttingen, Germany, 1997. (b) Farrugia, L. J. *WinGX*; University of Glasgow: Glasgow, Great Britain, 1998.
(12) (a) Meiser, C.; Song, B.; Freisinger, E.; Peilert, M.; Sigel, H.; Lippert, B. *Chem.—Eur. J.* **1997**, *3*, 388–398. (b) Raudaschl-Sieber, G.; Schöllhorn, H.; Thewalt, U.; Lippert, B. *J. Am. Chem. Soc.* **1985**, *107*, 3591–3595.
(13) Jaworski, S.; Menzer, S.; Lippert, B.; Sabat, M. *Inorg. Chim. Acta* **1993**, *205*, 31–34.
(14) Prater, M. E.; Mindiola, D. J.; Ouyang, X.; Dunbar, K. R. *Inorg. Chem. Commun.* **1998**, *1*, 475–477.
(15) See, e.g., (a) Beer, P. D.; Hayes, E. J. *Coord. Chem. Rev.* **2003**, *240*, 167–189. (b) Bondy, C. R.; Gale, P. A.; Loeb, S. J. *J. Am. Chem. Soc.* **2004**, *126*, 5030–5031. (c) Tovilla, J. A.; Vilar, R.; White, A. J. P. *Chem. Commun.* **2005**, 4839–4841. (d) Amendola, V.; Fabbrizzi, L. *Chem. Commun.* **2009**, 513–531. (e) Galstyan, A.; Sanz Miguel, P. J.; Lippert, B. *Chem.—Eur. J.* **2010**, *16*, 5577–5580.
(16) For discussions on relationship between torsional angles and M···M distances in dinuclear Pt complexes: (a) Hollis, L. S.; Lippard, S. J. *Inorg. Chem.* **1983**, *22*, 2600–2604. (b) Schöllhorn, H.; Thewalt, U.; Lippert, B. *Inorg. Chim. Acta* **1984**, *93*, 19–26.
(17) Trovó, G.; Bandoli, G.; Nicolini, M.; Longato, B. *Inorg. Chim. Acta* **1993**, *211*, 95–99.
(18) Bivián-Castro, E. Y.; Roitzsch, M.; Gupta, D.; Lippert, B. *Inorg. Chim. Acta* **2005**, *358*, 2395–2402.
(19) Kistenmacher, T. J.; Rossi, M. *Acta Crystallogr.* **1977**, *B33*, 253–256.
(20) (a) Taylor, R.; Kennard, O. *J. Mol. Struct.* **1982**, *78*, 1–28. (b) Clowney, L.; Jain, S. C.; Srinivasan, A. R.; Westbrook, J; Olson, W. K.; Berman, H. M. *J. Am. Chem. Soc.* **1996**, *118*, 509–518.
(21) (a) Frey, M. N.; Koetzle, T. F.; Lehmann, M. S.; Hamilton, W. C. *J. Chem. Phys.* **1973**, *59*, 915–924. (b) McMullan, R. K.; Benci, P.; Craven, B. M. *Acta Crystallogr.* **1980**, *B36*, 1424–1430.
(22) Significance levels are 3.1−4.6σ with σ defined as $\sigma = (\sigma_1^2 + \sigma_2^2)^{1/2}$ and σ_1 representing the errors in interatomic distances to be compared.
(23) (a) Arpalahti, J.; Klika, K. D. *Eur. J. Inorg. Chem.* **1999**, 1199–1201. (b) Arpalahti, J.; Klika, K. D. *Eur. J. Inorg. Chem.* **2003**, 4195–4201.
(24) Yin, L.; Sanz Miguel, P. J.; Shen, W.-Z; Lippert, B. *Chem.—Eur. J.* **2009**, *15*, 10723–10726.
(25) The large C6−N6−Pd angles of 135.7(7)° (**4**) and 128.7(9)° and 130.3(9)° (**5**) are not inconsistent with this view.
(26) Krumm, M.; Mutikainen, I.; Lippert, B. *Inorg. Chem.* **1991**, *30*, 884–890.
(27) Interestingly, the isotopic exchange of the H8 resonance of the 9-methyladeninato ligands in **5** is markedly slower than that in **4**.
(28) O'Halloran, T. V.; Lippard, S. J. *Inorg. Chem.* **1989**, *28*, 1289–1295.
(29) Iwatsuki, S.; Itou, T.; Ito, H.; Mori, H.; Uemura, K.; Yokomori, Y.; Ishihara, K.; Matsumoto, K. *Dalton Trans.* **2006**, 1497–1504.
(30) See, e.g., (a) Vestues, P. I.; Martin, R. B. *J. Am. Chem. Soc.* **1981**, *103*, 806–809. (b) Scheller, K. H.; Scheller-Krattiger, V.; Martin, R. B. *J. Am. Chem. Soc.* **1981**, *103*, 6833–6839. (c) Häring, U. K.; Martin, R. B. *Inorg. Chim. Acta* **1983**, *78*, 259–267.
(31) Mahoney, D. F.; Beattie, J. K. *Inorg. Chem.* **1973**, *12*, 2561–2565.
(32) (a) Jeong, K. S.; Kim, S. Y.; Shin, U.-S.; Kogej, M.; Hai, N. T. M.; Broekmann, P.; Jeong, N.; Kirchner, B.; Reiher, M.; Schalley, C. A. *J. Am. Chem. Soc.* **2005**, *127*, 17672–17685. (b) Bardají, E. G.; Freisinger, E.; Costisella, B.; Schalley, C. A.; Brüning, W.; Sabat, M.; Lippert, B. *Chem.—Eur. J.* **2007**, *13*, 6019–6039. (c) Holland, L.; Shen, W.-Z.; von Grebe, P.; Sanz Miguel, P. J.; Pichierri, F.; Springer, A.; Schalley, C. A.; Lippert, B. *Dalton Trans.* **2011**, *40*, 5159–5161.
(33) Lim, M. C.; Martin, R. B. J. *Inorg. Nucl. Chem.* **1976**, *38*, 1911–1914.
(34) Kampf, G; Sanz Miguel, P. J.; Morell Cerdà, M.; Willermann, M.; Schneider, A.; Lippert, B. *Chem.—Eur. J.* **2008**, *14*, 6882–6891.
(35) Komeda, S.; Lin, Y.-L.; Chikuma, M. *Chem. Med. Chem.* **2011**, *6*, 987–990 and references cited.
(36) For Ag^+ binding to N3 of 9-RA, see (a) Verma, S.; Mishra, A. K.; Kumar, J. *Acc. Chem. Res.* **2010**, *43*, 79–91. (b) Purohit, C. S.; Verma, S. *J. Am. Chem. Soc.* **2006**, *128*, 400–401. (c) Rother, I. B.; Freisinger, E.; Erxleben, A.; Lippert, B. *Inorg. Chim. Acta* **2000**, *300*−*302*, 339–352.
(37) $(PR_3)_2Pt^{II}$ triangle: Longato, B.; Pasquato, L.; Mucci, A.; Schenetti, L.; Zangrando, E. *Inorg. Chem.* **2003**, *42*, 7861–7871.